

On the Achievable Rate of a Sample-based Practical Photon-counting Receiver

Zhimeng Jiang, Chen Gong, Guanchu Wang, and Zhengyuan Xu

Abstract

We investigate the achievable rate for a practical receiver under on-off keying modulation based on Kullback-Leibler (KL) divergence and Chernoff α -divergence. The asymptotic tightness of the derived bounds is analyzed for large symbol duration and large peak power. We prove the tightness of the derived bounds for large symbol duration, large peak power with zero background radiation with exponential convergence rate, and for low peak power of order two. For large peak power with fixed background radiation and low background radiation with fixed peak power, the proposed bound gap is a small positive value for low background radiation and large peak power, respectively. Moreover, we propose an approximation on the achievable rate in the low background radiation and large symbol duration regime, which is more accurate compared with the derived upper and lower bounds in the medium signal to noise ratio (SNR) regime. The proposed bounds and the approximations are evaluated by the numerical results.

Key Words: Optical wireless communications, achievable rate, on-off keying modulation, dead time, finite sampling rate.

I. INTRODUCTION

On some specific occasions where the conventional RF is prohibited and direct link transmission cannot be guaranteed, non-line-of-sight (NLOS) optical scattering communication can be adopted to provide certain information transmission rate [1]. Optical scattering communication is typically developed in the ultraviolet (UV) spectrum due to solar blind region (200nm-280nm)

This work was supported by Key Program of National Natural Science Foundation of China (Grant No. 61631018) and Key Research Program of Frontier Sciences of CAS (Grant No. QYZDY-SSW-JSC003).

The authors are with Key Laboratory of Wireless-Optical Communications, Chinese Academy of Sciences, University of Science and Technology of China, Hefei, Anhui 230027, China. Email: {zhimengj, hegsns}@mail.ustc.edu.cn, {cgong821, xuzy}@ustc.edu.cn.

where the solar background radiation is negligible [1]. On the UV scattering communication channel characterization, extensive studies based on Monte Carlo simulation [2], [3], theoretical analysis [4], [5], [6] and experimental results [7], [8], [9] show that the atmospheric attenuation among scattering channel can be extremely large, especially for long-range transmission. Hence, it is difficult to detect the received signals using conventional continuous waveform receiver, such as photon-diode (PD) and avalanche photon-diode (APD). Instead, a photon-counting receiver is widely deployed.

For photon-counting receiver, the received signals are usually characterized by discrete photoelectrons, whose number in a certain interval satisfies a Poisson distribution. For such a Poisson channel, recent works mainly focus on the channel capacity, such as the continuous Poisson channel capacity [10], [11], discrete Poisson channel capacity [12], [13], as well as the Poisson interference channel capacity [14]. Besides, the system characterization and optimization, as well as the signal processing [15], [16], [17], [18], [19] have also been extensively studied from the receiver side.

Most information theoretical and signal processing works assume perfect photon-counting receiver, which is difficult to realize. A practical photon-counting receiver typically consists of a photomultiplier tube (PMT) as well as the subsequent sampling and processing blocks [20]. Recently, extensive efforts have been made to design and characterize practical photon-counting receivers, such as single photon avalanche diode (SPAD), which has been applied in many optical communication scenarios [21], [22]. In optical scattering communication, we consider a practical photon-counting receiver typically consists of a photomultiplier tube (PMT) and the subsequent pulse-holding circuits to generate a series of rectangular pulses with certain width. The square pulses generated by pulse-holding circuits typically have positive width that incurs dead time effect [23], where a photon arriving during the pulse duration of the previous photon cannot be detected due to the merge of two pulses. The dead time effect and the model of sub-Poisson distribution for the photon-counting processing have been investigated in [24], [25], where the variance is lower than its mean. The photon-counting system with dead time effect for infinite sampling rate has been investigated in optical communication for channel

characterizations [26], [27], optical wireless communications using SPAD detector [28], [29] and experimental implementation [21], [30]. The photon-counting system with dead time effect for finite sampling rate with shot noise of PMTs is investigated in [31] based on a rising-edge detector. However, the performance analysis for a sampling-based detector focusing on the achievable transmission rate is still missing.

In this work, we analyze the achievable rate of a sampling-based detector under positive dead time and finite sampling rate, assuming negligible electrical thermal noise and shot noise. We first derive the upper and lower bounds on the achievable rate based on Kullback-Leibler (KL) divergence and Chernoff α -divergence between the two symbols, respectively, with respect to three important parameters, the number of samples per symbol, the peak power, and the background radiation intensities. We investigate the convergence rate of the proposed upper and lower bounds. We demonstrate that the bound gap converges to zero with exponential rate for large sampling number L , large peak power A and zero background radiation Λ_0 . For low peak power A , the bound gap converges to zero with order A^2 . For large peak power A with fixed background radiation Λ_0 and low background radiation Λ_0 with fixed peak power A , the bound gap converges to certain small positive value for low background radiation Λ_0 and large peak power A , respectively.

The remainder of this paper is organized as follows. In Section II, we characterize the system model of the practical photon-counting receiver and achievable rate with on-off keying (OOK) modulation. In Section III, we derive the upper and lower bounds on the maximum achievable rate and demonstrate the asymptotic tightness. In Section IV, we investigate the asymptotic tightness of the upper and lower bounds for five scenarios. An approximation on the achievable rate is proposed for the medium signal to noise ratio (SNR) regime in Section V. Numerical results are shown in Section VI. Finally, we conclude this paper in Section VII.

II. SYSTEM MODEL

We introduce the following notations that will be adopted throughout this paper. Random variables and vectors are denoted by upper-case letters and bold uppercase letters, respectively. We use notation $Z_{[j]}$ to denote a sequence of random variables $\{Z_1, Z_2, \dots, Z_j\}$. Realizations of

random variables and random processes are denoted in lowercase letters, and follow the above notation conventions.

Consider single-user communication with a non-perfect receiver. Let $\Lambda(t)$ denote the \mathbb{R}_0^+ -valued photon arrival rate at time t , and

$$Y(t) = \mathcal{P}\left(\Lambda(t) + \Lambda_0\right), \quad (1)$$

denote the Poisson photon arrival process at the receiver, where Λ_0 is the background radiation arrival intensities, and $\mathcal{P}(\cdot)$ is the Poisson arrival process that records the time instants and number of photon arrivals. Let $N_{t-\tau,t}$ denote the number of photons arriving at the receiver during time interval $[t - \tau, t]$, satisfying the following probability,

$$\mathbb{P}\{N_{t-\tau,t} = k\} = \frac{1}{k!} e^{-\lambda_{t-\tau,t}} (\lambda_{t-\tau,t})^k, \quad k = 0, 1, \dots, \quad (2)$$

where $\lambda_{t-\tau,t} = \int_{t-\tau}^t \Lambda(t') dt'$. We consider peak power constraint, i.e., photon arrival rate $\Lambda(t)$ must satisfy the following constraint:

$$0 \leq \Lambda(t) \leq A, \quad (3)$$

where upper bound A is related to the maximum transmission power. Assume OOK modulation with symbol interval T_b , where $\Lambda(t) = A$ for symbol one and $\Lambda(t) = 0$ for symbol zero. Let $X_i \in \{0, 1\}$ denote the symbol in the i^{th} slot, which is independent across different time slots. Then, the arrival rate $\Lambda(t) = \sum_{i=0}^{+\infty} X_i A \cdot \mathbb{1}\{(i-1)T_b \leq t < iT_b\}$, where $\mathbb{1}\{\cdot\}$ is an indicator function. Further assume that X_i is independent and identically distributed for each i with probability $\mathbb{P}(X_i = 1) = \mu$. In the remainder of this paper, since we are interested in the achievable rate and symbols X_i are independent, we consider one symbol interval and omit subscript i .

Consider a practical receiver with finite sampling rate consisting of a PMT detector, an ADC, and a digital signal processor (DSP) unit. When a photon arrives, the PMT detector generates a pulse with certain width, which causes the merge of two pulses if the interval of two photon arrival instant is shorter than the pulse width. The maximum arrival time interval where the two pulses merge is called dead time, denoted as τ . Denote T_s as the ADC sampling interval

and assume low to medium sampling rate such that $T_s \geq \tau$. Considering the PMT sampling sequence in a symbol interval $Z_{[L]} = \{Z_1, \dots, Z_L\}$, where $L \triangleq \lfloor \frac{T}{T_s} \rfloor$, $\lfloor \cdot \rfloor$ is the lower rounding function. Note that for any $\tau > 0$, the number of photon arrivals $N_{0,\tau}$ on $[0, \tau]$ together with the corresponding (ordered) arrival time instants $\mathbb{T}^{N_\tau} = (T_1, \dots, T_{N_\tau})$ are complete descriptions of random process $Y_{0,\tau}$. According to above statement, we have

$$Z_i = \begin{cases} 0, & T_j \notin (iT_s - \tau, iT_s], \quad \forall j = 1, \dots, N_T; \\ 1, & \text{otherwise;} \end{cases} \quad (4)$$

$$\mathbb{P}(Z_i = 1) = 1 - e^{-(X_i A + \Lambda_0)\tau}. \quad (5)$$

In other words, Z_i is an indicator on whether one or more photons arrive within τ prior to the sampling instant. We call such equivalent channel *binominal channel*.

Consider the achievable rate for the above communication system. Let p_0 and p_1 denote probability $\mathbb{P}(Z_i = 1)$ for symbol $X = 0$ and $X = 1$, respectively. As the sum of variables with i.i.d. binary distribution is a sufficient statistic for these variables, we define summation $\hat{N} \triangleq \sum_{i=1}^L Z_i$ and the achievable rate is given as follows,

$$I(X; \hat{N}) = H(\hat{N}) - H(\hat{N}|X), \quad (6)$$

where \hat{N} follows binomial distributions $\mathbb{B}(p_0, L)$ and $\mathbb{B}(p_1, L)$ for symbol $X = 0$ and $X = 1$, respectively, and $\mathbb{B}(p, L)$ denotes binomial distribution with probability p for each trial and L trials.

III. THE BOUND ON MUTUAL INFORMATION

The mutual information involves the entropy of mixture distribution with intractable analytical form. Thus, pairwise-distances are adopted to provide the lower bound and upper bound on the mutual information [32]. The results are shown in the following proposition for completeness.

Proposition 1: Define X as the transmitted signal with measurable supports $\{x_1, \dots, x_n\}$ and $\mathbb{P}(X = x_i) \triangleq c_i$ for $i = 1, \dots, n$. The channel transition probability $\mathbb{P}(Y|X)$ can be represented by a set of distribution $\{p_1, \dots, p_n\}$, where $p_i(y) \triangleq \mathbb{P}(Y = y|X = x_i)$ for $i = 1, \dots, n$. We have the following lower bound and upper bound on mutual information $I(X; Y)$,

$$-\sum_{i=1}^n c_i \ln \sum_{j=1}^n c_j \exp(-C_\alpha(p_i||p_j)) \leq I(X; Y) \leq -\sum_{i=1}^n c_i \ln \sum_{j=1}^n c_j \exp(-KL(p_i||p_j)), \quad (7)$$

where Chernoff α -divergence $C_\alpha(p||q) = -\ln \int p^\alpha(y)q^{1-\alpha}(y)dy$ and Kullback-Leibler divergence $KL(p||q) = \int p(y) \ln \frac{p(y)}{q(y)}dy$.

Consider OOK modulation at the transmitter and photon-counting detection at the receiver. As $T_s \geq \tau$, the samples are mutually independent and photon-counting detection is performed via examining whether each sample is higher than a certain threshold. Assume negligible shot and thermal noise such that each sample can distinguish whether photons arrived or not perfectly. Let $p_i = 1 - e^{-(iA+\Lambda_0)\tau}$ for $i = 0$ and 1. Recalling that $\hat{N} \sim \mathbb{B}(L, p_i) \triangleq P_i^B(\cdot)$, the Chernoff α -divergence and KL divergence are given by

$$\begin{aligned} C_\alpha(P_1^B||P_0^B) &= -\ln \sum_{i=1}^n \binom{L}{i} (p_1^\alpha p_0^{1-\alpha})^i [(1-p_1)^\alpha (1-p_0)^{1-\alpha}]^{L-i} \\ &= -L \ln \left(p_1^\alpha p_0^{1-\alpha} + (1-p_1)^\alpha (1-p_0)^{1-\alpha} \right) = C_{1-\alpha}(P_0^B||P_1^B), \end{aligned} \quad (8)$$

$$\begin{aligned} KL(P_1^B||P_0^B) &= \sum_{i=0}^L \binom{L}{i} p_1^i (1-p_1)^{L-i} \left(i \ln \frac{p_1}{p_0} + (L-i) \ln \frac{1-p_1}{1-p_0} \right) \\ &= L \left(p_1 \ln \frac{p_1}{p_0} + (1-p_1) \ln \frac{1-p_1}{1-p_0} \right). \end{aligned} \quad (9)$$

Note that mutual information $I(X; \hat{N})$ depends on Λ_0 , A , L , μ and τ . Since $I(X; \hat{N}) = 0$ for $\mu = 0$ or $\mu = 1$, we focus on the maximum mutual information $I(X; \hat{N})$ over $\mu \in [0, 1]$ given fixed dead time τ . Define $I_{max}(\Lambda_0, A, L) \triangleq \max_{\mu \in [0, 1]} I(X; \hat{N})$. In the remainder of this Section, we investigate the lower and upper bounds on $I_{max}(\Lambda_0, A, L)$ and the asymptotic properties for large L and A .

A. Lower Bound on Mutual Information

According to Proposition 1, the lower bound on $I(X; \hat{N})$ is given as

$$\begin{aligned} I(X; \hat{N}) \geq & -\left\{ \mu \ln[(1-\mu) \exp(-C_\alpha(P_1^B||P_0^B)) + \mu] \right. \\ & \left. + (1-\mu) \ln[\mu \exp(-C_\alpha(P_0^B||P_1^B)) + (1-\mu)] \right\}. \end{aligned} \quad (10)$$

Note that the right-hand side of equation (10) increases with respect to $C_\alpha(P_1^B||P_0^B)$ and $C_\alpha(P_0^B||P_1^B)$, where the optimal α to maximize the right-hand side is intractable. We resort to a suboptimal solution to α , given as follows,

$$\alpha^* \triangleq \arg \max_{0 \leq \alpha \leq 1} \min\{C_\alpha(P_1^B||P_0^B), C_\alpha(P_0^B||P_1^B)\}. \quad (11)$$

We have the following Lemma 1 on optimal α^* .

Lemma 1: The optimal solution to problem (11), denoted as α^* , is $\frac{1}{2}$.

Proof: Please refer to Appendix VIII-A. ■

Define $\beta \triangleq e^{-C_{\alpha^*}(P_0^B||P_1^B)} = e^{-C_{\alpha^*}(P_1^B||P_0^B)} = (\sqrt{p_0 p_1} + \sqrt{(1-p_0)(1-p_1)})^L < 1$ and function $F_l(\mu, \beta) \triangleq -\{\mu \ln[(1-\mu)\beta + \mu] + (1-\mu) \ln[\mu\beta + (1-\mu)]\}$. We aim to maximize $F_l(\mu, \beta)$ with respect to μ to tighten the lower bound on $I(X; \hat{N})$. Since

$$\frac{\partial F_l}{\partial \mu} = \ln[1 - (1-\beta)\mu] - \frac{\beta}{1 - (1-\beta)\mu} - \{\ln[\beta + (1-\beta)\mu] - \frac{\beta}{\beta + (1-\beta)\mu}\}, \quad (12)$$

we have

$$\left. \frac{\partial F_l}{\partial \mu} \right|_{(0,\beta)} = -\ln \beta + 1 - \beta > 0, \quad \left. \frac{\partial F_l}{\partial \mu} \right|_{(1,\beta)} = \ln \beta - 1 + \beta < 0, \quad (13)$$

$$\frac{\partial^2 F_l}{\partial \mu^2} = -\frac{1-\beta}{1-(1-\beta)\mu} - \frac{\beta(1-\beta)}{(1-(1-\beta)\mu)^2} - \frac{1-\beta}{\beta+(1-\beta)\mu} - \frac{\beta(1-\beta)}{(\beta+(1-\beta)\mu)^2} < 0. \quad (14)$$

Thus, the optimal μ maximizing $F_l(\mu)$ uniquely exists and satisfies $\frac{\partial F_l}{\partial \mu} = 0$. Define monotonic increasing function $G(x) \triangleq \ln x - \frac{\beta}{x}$. Since $\left. \frac{\partial F_l}{\partial \mu} \right|_{(\mu^*, \beta)} = G(1-(1-\beta)\mu^*) - G(\beta+(1-\beta)\mu^*) = 0$, we have $1-(1-\beta)\mu^* = \beta+(1-\beta)\mu^*$ and $\mu^* = \frac{1}{2}$. Thus, we have the following lower bound,

$$I_{max}(\Lambda_0, A, L) \geq \max_{\mu \in [0,1]} F_l(\mu, \beta) = -\ln \frac{1+\beta}{2}. \quad (15)$$

B. Upper Bound on Mutual Information

The upper bound can be obtained using similar method as that of obtaining the lower bound. Defining $\beta_1 \triangleq \exp(-KL(P_1^B||P_0^B))$ and $\beta_2 \triangleq \exp(-KL(P_0^B||P_1^B))$, we have the following,

$$F_u(\mu, \beta_1, \beta_2) = -\{\mu \ln[(1-\mu)\beta_1 + \mu] + (1-\mu) \ln[\mu\beta_2 + (1-\mu)]\}, \quad (16)$$

$$KL(P_1^B||P_0^B) - KL(P_0^B||P_1^B) = (p_1 - p_0) \ln \frac{p_1(1-p_1)}{p_0(1-p_0)} \stackrel{\leq}{\geq} 0, \quad \text{if } p_0 + p_1 \stackrel{\geq}{\leq} 1. \quad (17)$$

Define $\mu^*(\beta_1, \beta_2) \triangleq \arg \max_{0 \leq \mu \leq 1} F_u(\mu, \beta_1, \beta_2)$. Although closed form of $\mu^*(\beta_1, \beta_2)$ is intractable, we have the following properties on $\mu^*(\beta_1, \beta_2)$,

Lemma 2: Cycle $\mu^*(\beta_1, \beta_2)$ must satisfy the following properties,

- (1) $\mu^*(\beta_1, \beta_2) + \mu^*(\beta_2, \beta_1) = 1$. Particularly, $\mu^*(\beta_1, \beta_2) = \frac{1}{2}$ if $\beta_1 = \beta_2$.
- (2) $\mu^*(\beta_1, \beta_2) \geq \frac{1-\beta_1}{2-\beta_1-\beta_2}$ if $\beta_1 \geq \beta_2$.

Proof: Please refer to Appendix VIII-B. ■

Lemma 3: We have that

$$\max_{0 \leq \mu \leq 1} F_u(\mu, \beta_1, \beta_2) \leq \frac{|\beta_1 - \beta_2|(1 - \min\{\beta_1, \beta_2\})}{1 - \beta_1\beta_2} - \ln \frac{1 - \beta_1\beta_2}{2 - \beta_1 - \beta_2}, \quad (18)$$

where equality holds if and only if $\beta_1 = \beta_2$.

Proof: Please refer to Appendix VIII-C. ■

According to Lemma 3, an upper bound on the maximal mutual information is given by,

$$I_{max}(\Lambda_0, A, L) \leq \max_{\mu \in [0,1]} F_u(\mu, \beta_1, \beta_2) \leq \frac{|\beta_1 - \beta_2|(1 - \min\{\beta_1, \beta_2\})}{1 - \beta_1\beta_2} - \ln \frac{1 - \beta_1\beta_2}{2 - \beta_1 - \beta_2}. \quad (19)$$

The above discussions can be summarized into the following result.

Theorem 1: We have that lower and upper bounds on $I_{max}(\Lambda_0, A, L)$ are given by Equations (15) and (19), respectively.

C. Asymptotic Mutual Information

We first provide an interpretation to show the tightness of the upper and lower bounds. By applying Jensens inequality to Chernoff α -divergence, we have

$$C_\alpha(P_0^B || P_1^B) = -\ln \mathbb{E}_{P_0^B} \left[\left(\frac{P_1^B}{P_0^B} \right)^{1-\alpha} \right] \leq -\int P_0^B \ln \left(\frac{P_1^B}{P_0^B} \right)^{1-\alpha} dx = (1-\alpha)KL(P_0^B || P_1^B) \quad (20)$$

$$C_\alpha(P_0^B || P_1^B) = -\ln \mathbb{E}_{P_1^B} \left[\left(\frac{P_0^B}{P_1^B} \right)^\alpha \right] \leq -\int P_1^B \ln \left(\frac{P_0^B}{P_1^B} \right)^\alpha dx = \alpha KL(P_1^B || P_0^B), \quad (21)$$

i.e., $C_{\frac{1}{2}}(P_0^B || P_1^B) \leq \frac{1}{2} \min\{KL(P_0^B || P_1^B), KL(P_1^B || P_0^B)\}$. Thus we have

$$\exp(-C_{\frac{1}{2}}(P_0^B || P_1^B)) > \exp(-2C_{\frac{1}{2}}(P_0^B || P_1^B)) \geq \exp(-\min\{KL(P_0^B || P_1^B), KL(P_1^B || P_0^B)\}), \quad (22)$$

i.e., $\beta > \beta^2 \geq \max\{\beta_1, \beta_2\}$. We consider two cases, large $C_\alpha(P_0^B || P_1^B)$ and negligible $\max\{KL(P_1^B || P_0^B), KL(P_0^B || P_1^B)\}$. **Define high SNR for negligible β and low SNR if β_1 and β_2 approach 1, which agrees with the true scenarios of high SNR and low SNR in the physical communication channel.** Note that for high SNR regime, β , β_1 and β_2 approach 0; and for low SNR regime, β , β_1 and β_2 approach 1, i.e., β and (β_1, β_2) contributes similarly to the lower and upper bounds. Thus, lower bound (15) and upper bound (19) validate in both high and low SNR regimes.

As the asymptotic maximum mutual information approaches 0 in low SNR regime, we focus on high SNR regime, including large L and A . For large L , we have the following Theorem 2 on the asymptotic results of the maximum mutual information.

Theorem 2: For large L , the asymptotic maximum mutual information is given by

$$I_{max}(\Lambda_0, A, L) \begin{cases} \geq \ln 2 - \beta + o(\beta), & \forall \beta_1, \beta_2; \\ \leq \ln 2 - \beta_1, & \beta_1 = \beta_2; \\ \leq \ln 2 + \frac{\max\{\beta_1, \beta_2\}}{2} + o(\max\{\beta_1, \beta_2\}), & \beta_1 \neq \beta_2; \end{cases} \quad (23)$$

where $\beta = \exp\left(L \ln\left(\sqrt{p_0 p_1} + \sqrt{(1-p_0)(1-p_1)}\right)\right)$, $\beta_1 = \exp\left(-L\left(p_1 \ln \frac{p_1}{p_0} + (1-p_1) \ln \frac{1-p_1}{1-p_0}\right)\right)$ and $\beta_2 = \exp\left(-L\left(p_0 \ln \frac{p_0}{p_1} + (1-p_0) \ln \frac{1-p_0}{1-p_1}\right)\right)$.

Proof: Please refer to Appendix VIII-D. ■

Theorem 2 implies that the asymptotic maximum mutual information $\lim_{L \rightarrow \infty} I_{max}(\Lambda_0, A, L) = \ln 2$. For large peak power A , we have the following expansions on β , β_1 , β_2 .

Lemma 4: For large A , the expansion on β , β_1 and β_2 are given by

$$\begin{aligned} \beta &= \left(\sqrt{p_0 p_1} + \sqrt{(1-p_0)(1-p_1)}\right)^L \\ &= p_0^{\frac{L}{2}} - p_0^{\frac{L-1}{2}} \left(\frac{\sqrt{p_0}}{2}(1-p_1) - \sqrt{(1-p_0)(1-p_1)}^{\frac{1}{2}}\right) + o(1-p_1); \end{aligned} \quad (24)$$

$$\begin{aligned} \beta_1 &= \left(\frac{p_0}{p_1}\right)^{p_1 L} \left(\frac{1-p_0}{1-p_1}\right)^{(1-p_1)L} \\ &= p_0^L - p_0^L \left(-L(1-p_1) + (1-p_1)L \ln \frac{1-p_1}{1-p_0}\right) + o(1-p_1); \end{aligned} \quad (25)$$

$$\begin{aligned} \beta_2 &= \left(\frac{p_1}{p_0}\right)^{p_0 L} \left(\frac{1-p_1}{1-p_0}\right)^{(1-p_0)L} \\ &= \left(\frac{1}{p_0}\right)^{p_0 L} \left(\frac{1}{1-p_0}\right)^{(1-p_0)L} (1-p_1)^{(1-p_0)L} + o(1-p_1). \end{aligned} \quad (26)$$

Proof: Please refer to Appendix VIII-E. ■

Noting that $1-p_1 = \exp(-(A + \Lambda_0)\tau)$, Lemma 4 shows the expansions of β , β_1 and β_2 with exponential convergence for large A . Furthermore, we have the following Theorem 3 on the asymptotic maximum mutual information.

Theorem 3: For large A , the asymptotic maximum mutual information is given by

$$I_{max}(\Lambda_0, A, L) \geq \ln \frac{2}{1+p_0^{\frac{L}{2}}} + \frac{p_0^{\frac{L-1}{2}}}{1+p_0^{\frac{L}{2}}} \left(\frac{\sqrt{p_0}}{2}(1-p_1) - \sqrt{(1-p_0)(1-p_1)}^{\frac{1}{2}}\right) + o(1-p_1), \quad (27)$$

$$I_{max}(\Lambda_0, A, L) \leq p_0^L + \ln(2-p_0^L) + O(\max\{(1-p_1) \ln(1-p_1), (1-p_1)^{(1-p_0)L}\}). \quad (28)$$

Proof: Please refer to Appendix VIII-F. ■

Theorem 3 shows the upper and lower bounds on the maximum mutual information as $\ln \frac{2}{1+p_0^{\frac{L}{2}}} \leq \lim_{A \rightarrow \infty} I_{max}(\Lambda_0, A, L) \leq p_0^L + \ln(2-p_0^L)$ for fixed Λ_0 . Specifically, we have the following

on the asymptotic maximum mutual information for zero Λ_0 ,

$$\lim_{A \rightarrow \infty} I_{max}(0, A, L) = \ln 2 = \lim_{L \rightarrow \infty} I_{max}(\Lambda_0, A, L). \quad (29)$$

IV. ASYMPTOTIC TIGHTNESS OF UPPER AND LOWER BOUND

Section III-C provides an interpretation on the tightness of bounds and show the asymptotic maximum mutual information for large L and A . However, the convergence rate of upper and lower bounds is still unknown. In this Section, we proceed to investigate the convergence rate of the upper and lower bounds.

Defining bound gap $\Delta(\beta, \beta_1, \beta_2) \triangleq \max_{\mu \in [0,1]} F_u(\mu, \beta_1, \beta_2) - F_l(\mu, \beta)$, we have the following Theorem 4 on the upper and lower bounds on $\Delta(\beta, \beta_1, \beta_2)$.

Theorem 4: For low SNR, we have the following upper bound on $\Delta(\beta, \beta_1, \beta_2)$,

$$\Delta(\beta, \beta_1, \beta_2) \leq \frac{1}{108} \left(\frac{\beta}{\beta_1} - 1 \right) \left(16 \frac{\beta}{\beta_1} + 11 \right) + \frac{1}{108} \left(\frac{\beta}{\beta_2} - 1 \right) \left(16 \frac{\beta}{\beta_2} + 11 \right); \quad (30)$$

and for high SNR, we have the following upper bound on $\Delta(\beta, \beta_1, \beta_2)$,

$$\Delta(\beta, \beta_1, \beta_2) \leq (\beta - \beta_1) + (\beta - \beta_2). \quad (31)$$

For general β, β_1, β_2 , we have the following lower bound on $\Delta(\beta, \beta_1, \beta_2)$,

$$\Delta(\beta, \beta_1, \beta_2) \geq \frac{1}{2} \ln \frac{1 + \beta}{1 + \beta_1} + \frac{1}{2} \ln \frac{1 + \beta}{1 + \beta_2}. \quad (32)$$

Proof: Please refer to Appendix VIII-G. ■

To characterize the convergence of $\Delta(\beta, \beta_1, \beta_2)$, we consider the *exponential rate* of convergence [33]. In summary, we consider five scenarios, where the convergence rates of the bound gap are shown in Table I.

A. Asymptotic Tightness of Bound Gap for Large L

As L approaches infinity, β, β_1 and β_2 approach 0, which corresponds to high SNR regime. Then, we have the following Theorem 5 on the convergence rate of bound gap $\Delta(\beta, \beta_1, \beta_2)$.

Theorem 5: As L approaches infinity, the convergence rate of gap $\Delta(\beta, \beta_1, \beta_2)$ is given by,

$$-\lim_{L \rightarrow \infty} \frac{\ln \Delta(\beta, \beta_1, \beta_2)}{L} = -\ln \left(\sqrt{p_0 p_1} + \sqrt{(1 - p_0)(1 - p_1)} \right), \quad (33)$$

Proof: Please refer to Appendix VIII-H. ■

Theorem 6 demonstrates that the proposed bounds is asymptotically tight, where bound gap $\Delta(\beta, \beta_1, \beta_2)$ approaches zero with exponential rate $-\ln \left(\sqrt{p_0 p_1} + \sqrt{(1 - p_0)(1 - p_1)} \right)$ as L approaches infinity.

TABLE I
THE CONVERGENCE RATE OF BOUND GAP FOR 5 SCENARIO.

Scenario	Convergence	Asymptotic tightness
Large L	$O\left(\exp\left(L \ln\left(\sqrt{p_0 p_1} + \sqrt{(1-p_0)(1-p_1)}\right)\right)\right)$	✓
Large A fixed Λ_0	$\geq \ln\left(1 + p_0^{\frac{L}{2}}\right) - \frac{1}{2} \ln\left(1 + p_0^L\right) + O\left(\exp\left(\min\left\{\frac{1}{2}, (1-p_0)L\right\}A\tau\right)\right)$ $\leq 2p_0^{\frac{L}{2}} - p_0^L + O\left(\exp\left(\min\left\{\frac{1}{2}, (1-p_0)L\right\}A\tau\right)\right)$	✗
Low Λ_0 fixed A	$\geq \ln\left(1 + (1-p_1)^{\frac{L}{2}}\right) - \frac{1}{2} \ln\left(1 + (1-p_1)^L\right) + O\left(\min\left\{\frac{1}{2}, p_1 L\right\}\Lambda_0\tau\right)$ $\leq 2(1-p_1)^{\frac{L}{2}} - (1-p_1)^L + O\left(\min\left\{\frac{1}{2}, p_1 L\right\}\Lambda_0\tau\right)$	✗
Large A fixed $\Lambda_0 = 0$	$O\left(\exp\left(-\frac{L\tau}{2}A\right)\right)$	✓
Low A fixed Λ_0	$O\left(\frac{3L(1-p_0)}{16p_0}\tau^2 A^2\right)$	✓

B. Bound Gap for Large Peak Power A

As peak power A approaches infinity, probability p_1 approaches 1 and β, β_1, β_2 approach 0, which also corresponds to high SNR regime. We have the following upper and lower bounds on the bound gap $\Delta(\beta, \beta_1, \beta_2)$.

Theorem 6: For large peak power and fixed background radiation arrival intensities, we have the following upper and lower bounds on $\Delta(\beta, \beta_1, \beta_2)$,

$$\Delta(\beta, \beta_1, \beta_2) \leq 2p_0^{\frac{L}{2}} - p_0^L + \epsilon_u + o(\epsilon_u), \quad (34)$$

$$\Delta(\beta, \beta_1, \beta_2) \geq \ln\left(1 + p_0^{\frac{L}{2}}\right) - \frac{1}{2} \ln\left(1 + p_0^L\right) + \epsilon_l + o(\epsilon_l), \quad (35)$$

where

$$\epsilon_u = \begin{cases} 2p_0^{\frac{L-1}{2}} \sqrt{1-p_0}(1-p_1)^{\frac{1}{2}}, & (1-p_0)L > \frac{1}{2}; \\ \left\{2p_0^{\frac{L-1}{2}} \sqrt{1-p_0} - p_0^{-L+\frac{1}{2}}(1-p_0)^{-\frac{1}{2}}\right\}(1-p_1)^{\frac{1}{2}}, & (1-p_0)L = \frac{1}{2}; \\ -p_0^{-Lp_0}(1-p_0)^{-L(1-p_0)}(1-p_1)^{L(1-p_0)}, & (1-p_0)L < \frac{1}{2}; \end{cases} \quad (36)$$

$$\epsilon_l = \begin{cases} (1+p_0^{\frac{L}{2}})^{-1} p_0^{\frac{L-1}{2}} \sqrt{1-p_0}(1-p_1)^{\frac{1}{2}}, & (1-p_0)L > \frac{1}{2}; \\ \left\{(1+p_0^{\frac{L}{2}})^{-1} p_0^{\frac{L-1}{2}} \sqrt{1-p_0} - \frac{1}{2} p_0^{-L+\frac{1}{2}}(1-p_0)^{-\frac{1}{2}}\right\}(1-p_1)^{\frac{1}{2}}, & (1-p_0)L = \frac{1}{2}; \\ -\frac{1}{2} p_0^{-Lp_0}(1-p_0)^{-L(1-p_0)}(1-p_1)^{L(1-p_0)}, & (1-p_0)L < \frac{1}{2}. \end{cases} \quad (37)$$

Proof: Please refer to Appendix VIII-I. ■

Theorem 6 demonstrates that the offset items ϵ_u and ϵ_l converge to 0 as peak power A approaches infinity. Furthermore, the exponential rates of ϵ_u and ϵ_l with respect to A are given

as follows,

$$-\lim_{A \rightarrow \infty} \frac{\ln \epsilon_u}{A} = \min\left\{\frac{1}{2}, (1-p_0)L\right\}\tau, \quad (38)$$

$$-\lim_{A \rightarrow \infty} \frac{\ln \epsilon_l}{A} = \min\left\{\frac{1}{2}, (1-p_0)L\right\}\tau. \quad (39)$$

When peak power A approaches infinity, the offset items are negligible for low p_0 , and the following is approximately satisfied,

$$\ln(1+p_0^{\frac{L}{2}}) - \frac{1}{2} \ln(1+p_0^L) \leq \Delta(\beta, \beta_1, \beta_2) \leq 2p_0^{\frac{L}{2}} - p_0^L. \quad (40)$$

C. Bound Gap for Low Background Noise Λ_0

For low background radiation arrival intensities, probability p_0 approaches 0 and β, β_1, β_2 approach 0, which corresponds to high SNR regime. We have the following upper and lower bounds on bound gap $\Delta(\beta, \beta_1, \beta_2)$.

Theorem 7: For low background radiation arrival intensities given fixed peak power, we have the following upper and lower bounds on $\Delta(\beta, \beta_1, \beta_2)$,

$$\Delta(\beta, \beta_1, \beta_2) \leq 2(1-p_1)^{\frac{L}{2}} - (1-p_1)^L + \epsilon'_u + o(\epsilon'_u), \quad (41)$$

$$\Delta(\beta, \beta_1, \beta_2) \geq \ln(1+(1-p_1)^{\frac{L}{2}}) - \frac{1}{2} \ln(1+(1-p_1)^L) + \epsilon'_l + o(\epsilon'_l), \quad (42)$$

where

$$\epsilon'_u = \begin{cases} 2(1-p_1)^{\frac{L-1}{2}} \sqrt{p_1 p_0^{\frac{1}{2}}}, & p_1 L > \frac{1}{2}; \\ \left\{ 2(1-p_1)^{\frac{L-1}{2}} \sqrt{p_1} - (1-p_1)^{-L+\frac{1}{2}} p_1^{-\frac{1}{2}} \right\} p_0^{\frac{1}{2}}, & p_1 L = \frac{1}{2}; \\ -(1-p_1)^{-L(1-p_1)} p_1^{-L p_1} p_0^{L p_1}, & p_1 L < \frac{1}{2}; \end{cases} \quad (43)$$

$$\epsilon'_l = \begin{cases} (1+(1-p_1)^{\frac{L}{2}})^{-1} (1-p_1)^{\frac{L-1}{2}} \sqrt{p_1 p_0^{\frac{1}{2}}}, & p_1 L > \frac{1}{2}; \\ \left\{ (1+(1-p_1)^{\frac{L}{2}})^{-1} (1-p_1)^{\frac{L-1}{2}} \sqrt{p_1} - \frac{1}{2} (1-p_1)^{-L+\frac{1}{2}} p_1^{-\frac{1}{2}} \right\} p_0^{\frac{1}{2}}, & p_1 L = \frac{1}{2}; \\ -\frac{1}{2} (1-p_1)^{-L(1-p_1)} p_1^{-L p_1} p_0^{L p_1}, & p_1 L < \frac{1}{2}. \end{cases} \quad (44)$$

Proof: According to reciprocities $p_0 \longleftrightarrow 1-p_1$, $p_1 \longleftrightarrow 1-p_0$ and Theorem 6, we can readily obtain the results in Theorem 7. The detailed procedure is omitted here. \blacksquare

Theorem 7 demonstrates that offset items ϵ'_u and ϵ'_l converge 0 as the background radiation arrival intensities Λ_b approaches 0. Furthermore, the linear convergence rate of ϵ'_u and ϵ'_l with

respect to Λ_b can be obtained as follows,

$$\lim_{\Lambda_b \rightarrow 0} \frac{\epsilon'_u}{\Lambda_b} = \min\left\{\frac{1}{2}, p_1 L\right\}\tau, \quad (45)$$

$$\lim_{\Lambda_b \rightarrow 0} \frac{\epsilon'_l}{\Lambda_b} = \min\left\{\frac{1}{2}, p_1 L\right\}\tau. \quad (46)$$

As background radiation arrival intensities Λ_b approaches 0, the gap is negligible for small Λ_b and the following is approximately satisfied,

$$\ln(1 + (1 - p_1)^{\frac{L}{2}}) - \frac{1}{2} \ln(1 + (1 - p_1)^L) \leq \Delta(\beta, \beta_1, \beta_2) \leq 2(1 - p_1)^{\frac{L}{2}} - (1 - p_1)^L. \quad (47)$$

D. Bound Gap for Large Peak Power A and $\Lambda_0 = 0$

For zero background radiation arrival intensities, we have probability $p_0 = 0$ and $\beta = (1 - p_1)^{\frac{L}{2}}$, $\beta_1 = 0$, $\beta_2 = (1 - p_1)^L$, which corresponds to high SNR regime. We have the following on bound gap $\Delta(\beta, \beta_1, \beta_2)$.

Theorem 8: For large peak power A and zero background radiation arrival intensities Λ_0 , we have the following on $\Delta(\beta, \beta_1, \beta_2)$,

$$-\lim_{A \rightarrow \infty} \frac{\ln \Delta(\beta, \beta_1, \beta_2)}{A} = \frac{L\tau}{2}. \quad (48)$$

Proof: Please refer to Appendix VIII-J. ■

Theorem 8 demonstrates that the upper and lower bounds are asymptotically tight for sufficiently large peak power A if background radiation arrival intensities $\Lambda_0 = 0$, with exponential rate $\frac{L\tau}{2}$.

E. Bound Gap for Low Peak Power A

For low peak power, probability p_1 approaches p_0 and β, β_1, β_2 approach 1, which corresponds to low SNR regime. We have the following result on bound gap $\Delta(\beta, \beta_1, \beta_2)$.

Theorem 9: For low peak power A given fixed background radiation arrival intensities Λ_0 , we have the following on $\Delta(\beta, \beta_1, \beta_2)$,

$$\Delta(\beta, \beta_1, \beta_2) = \frac{3L(1 - p_0)}{16p_0} \tau^2 A^2 + o(A^2). \quad (49)$$

Proof: Please refer to Appendix VIII-K. ■

Theorem 9 demonstrates that bound gap $\Delta(\beta, \beta_1, \beta_2)$ converges to 0 with order A^2 .

V. APPROXIMATE METHOD

For most scenarios of UV communication, background radiation arrival intensities Λ_0 is negligible. Since the proposed lower and upper bounds on $I(X; \hat{N})$ is loose in medium SNR regime, we propose an approximation method to characterize $I(X; \hat{N})$ in medium SNR regime. The approximated mutual information $I(X; \hat{N})$ based on low Λ_0 is shown in Theorem 10.

Theorem 10: For low background radiation arrival intensities Λ_0 , we have the following expansion on $I(X; \hat{N})$,

$$\begin{aligned}
 I(X; \hat{N}) &= -[\mu(1-p_1)^L + 1 - \mu] \ln[\mu(1-p_1)^L + 1 - \mu] + \mu L(1-p_1)^L \ln(1-p_1) \\
 &\quad - \mu[1 - (1-p_1)^L] \ln \mu + (1-\mu)Lp_0 \{\ln[\mu(1-p_1)^L + 1 - \mu] - \ln(\mu Lp_1) \\
 &\quad - (L-1) \ln(1-p_1)\} - (1-\mu)h_b(Lp_0) + o(Lp_0) + O\left(\frac{1}{L}\right). \tag{50}
 \end{aligned}$$

Proof: Please refer to Appendix VIII-L. ■

The approximation mutual information can be obtained from Equation (50) via omitting the terms with small o and big O . For reliable communication system, the sampling numbers L is typically large and background radiation arrival intensities Λ_0 is low. Thus, the proposed approximate mutual information can be adopted in the medium SNR regime.

VI. NUMERICAL AND SIMULATION RESULTS

Assume photon-counting receiver with OOK modulation. We adopt the following system parameters: symbol rate is set to 1MSPS; dead time 20ns [34]; background radiation arrival intensities $20000s^{-1}$, such that the normalized dead time is 0.02 and the normalized background photon rate is 0.02. For simplicity, we adopt normalized dead time, peak power, background radiation arrival intensities. We first investigate the optimal duty cycle for binominal channel by brute-force method (red full line), the suboptimal duty cycle by approximation based on Equation (50) (black full line), and the lower and upper bounds (blue and purple full line) with respect to peak power A , for $L = 20$ and $L = 30$ as shown in Figure 1 and Figure 2, respectively. It is seen that the optimal duty cycle and proposed suboptimal duty cycle from the derived lower and upper bound approach 0.5 as the peak power approaches infinity, i.e., the proposed suboptimal duty cycle from the derived lower and upper bounds is asymptotically optimal for large peak power. In addition, the proposed suboptimal duty cycle converges to optimal duty cycle faster

for a larger sampling number L . For large peak power and large L , the suboptimal duty cycle by approximation method is less accurate due to omitted larger coefficient one-order term in Equation (96) [35].

For mutual information, Figure 3 shows the mutual information of binominal channel, discrete Poisson channel, along with the derived upper and lower bounds and the approximation based on Equation (50) with respect to duty cycle. The normalized dead time, background noise, peak power and sampling numbers are set to 0.02, 0.02, 10 and 30, respectively. It is seen that proposed upper bound and lower bound are more accurate in low or large duty cycle and approximation is more accurate for medium and large duty cycle. The mutual information of discrete Poisson channel is also plotted as a benchmark to show the small loss due to imperfect receiver. “Lower bound opt” and “Lower bound” curves are obtained by brute-force search on α and suboptimal α in Lemma 1, respectively. Figure 4 shows the maximum mutual information over duty cycle μ with respect to peak power. The maximum mutual information with respect to duty cycle μ for binominal channel, approximation method, discrete Poisson channel, the lower bound and the upper bound are obtained by brute-force search, and that for “lower bound sub” and “upper bound sub” are obtained from Lemma 1 and Lemma 3, respectively. It is seen that proposed upper bound and lower bound become more accurate as peak power A increases, and the approximation is more accurate in low and medium peak power regimes.

Consider the asymptotic tightness of the proposed upper and lower bounds. The normalized dead time and background noise are both set to 0.02. We focus on the five scenarios addressed in Section IV. For large sampling numbers L , Figure 5 plots the bound gap by numerical method and the derived upper and lower bounds against sampling numbers L for different peak power values A . It is seen that the proposed upper and lower bounds on gap is becomes tighter as the peak power increases. Figure 6 shows the numerical values and the exponential term from Equation (33) of $\Delta(\beta, \beta_1, \beta_2)$ against sampling numbers L for different peak power values A . It is seen that the proposed upper and lower bounds converge to 0 with exponential rate as Equation (33) predicted. The normalized dead time and background noise are both set to 0.02.

Set the normalized dead time and sampling numbers to 0.1 and 10, respectively. For large peak

power A given fixed background radiation arrival intensities Λ_0 , Figure 7 plots the difference of derived upper and lower bounds on $\Delta(\beta, \beta_1, \beta_2)$ against peak power A for different background radiation arrival intensities Λ_0 , from both numerical computations and the limit from Equation (40) via omitting the vanishing terms. It is seen that the gap converges as A increases beyond 100. Figure 8 plots the offset items in the derived upper and lower bounds from Equations (34) and (35), respectively, against peak power A for different background radiation arrival intensities Λ_0 . The approximation values are obtained from the exponential terms. It is seen that the derived upper and lower bounds on the offset terms can well predict the true value with the same attenuation rate. In addition, the gap converges to 0 exponentially with the peak power.

Consider low background radiation arrival intensities Λ_0 given fixed peak power A , where the normalized dead time and sampling numbers are set to 0.1 and 10, respectively. Figure 9 plots the difference of derived upper and lower bounds on $\Delta(\beta, \beta_1, \beta_2)$ against background radiation arrival intensities Λ_0 for different peak power A . It is seen that the limit of the gap can well predict the true value. Figure 10 plots the offset item in the derived upper and lower bounds from Equations (41) and (42), against background radiation arrival intensities Λ_0 for different peak power A . It is seen that the offset items in the derived upper and lower bounds can well predict those from numerical computation. In addition, the gap between the numerical computation and theoretical approximation converges to 0 with linear rate for low peak power.

Consider large peak power A given background radiation arrival intensities $\Lambda_0 = 0$ where the normalized dead time and sampling numbers are set to 0.1, 10, respectively. Figure 11 plots the gap between derived upper and lower bounds on $\Delta(\beta, \beta_1, \beta_2)$ from Equations (84) and (85), respectively, against peak power A . It is seen that the gap from theoretical derivations can well predict the numerical results. The normalized dead time and sampling numbers are set to 0.1, 10, respectively. For low peak power A with the same normalized dead time and sampling numbers, Figure 12 plots the numerical values and theoretical approximations of the derived upper and lower bounds gap on $\Delta(\beta, \beta_1, \beta_2)$ against peak power A for different background radiation arrival intensities Λ_0 . It is seen that the approximation via dropping $o(A^2)$ item from Equation (49) can well predict that from numerical computation, which converges to 0 in the rate of order two

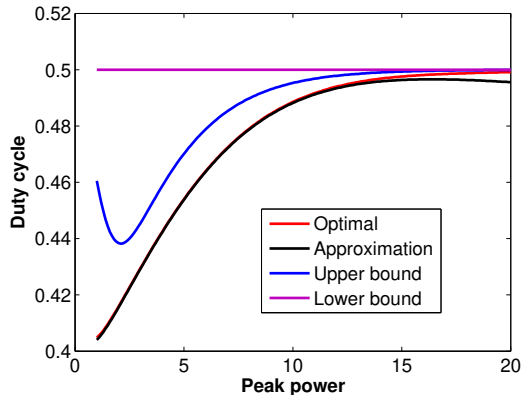


Fig. 1. The optimal/suboptimal duty cycle μ versus peak power A from brute-force approach, the derived bounds and approximation for $L = 20$.

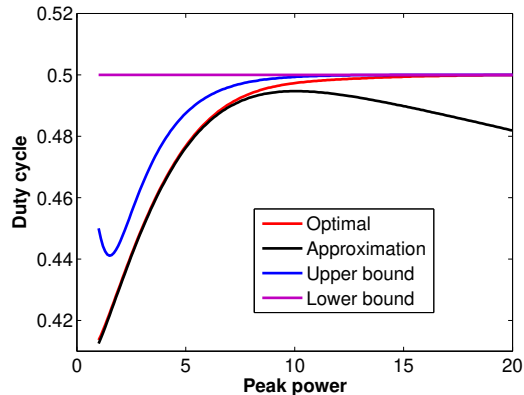


Fig. 2. The optimal/suboptimal duty cycle μ versus peak power A from the brute-force approach, the derived bounds and the approximation for $L = 30$.

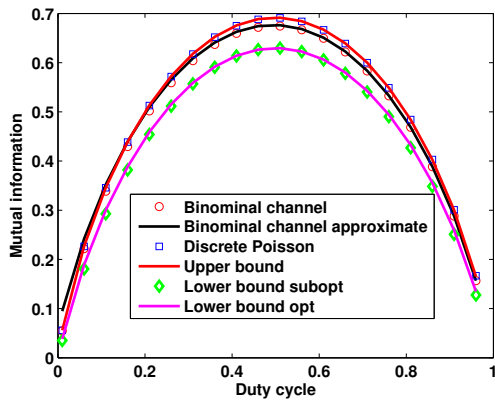


Fig. 3. The mutual information versus duty cycle μ from simulation, the derived bounds and approximation.

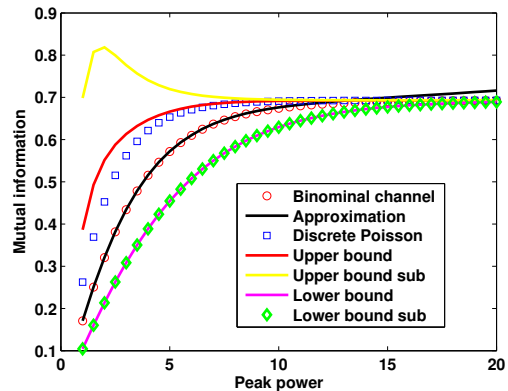


Fig. 4. The maximum mutual information over duty cycle μ versus peak power A from simulation, the derived bounds and approximation.

predicted by Equation (49) for low peak power.

VII. CONCLUSION

We have investigated the achievable rate of a photon counting receiver with positive dead time and finite sampling rate. We have proposed upper and lower bounds on the maximum achievable rate over duty cycle based on Kullback-Leibler (KL) divergence and Chernoff α -divergence, and shown the tightness of the proposed bounds. The convergence rate of proposed bounds is investigated for five scenarios. Moreover, an approximation on the achievable rate is proposed based on low background radiation, which is more accurate compared with the proposed upper and lower bounds in the medium signal to noise ratio (SNR) regime. The proposed upper/lower

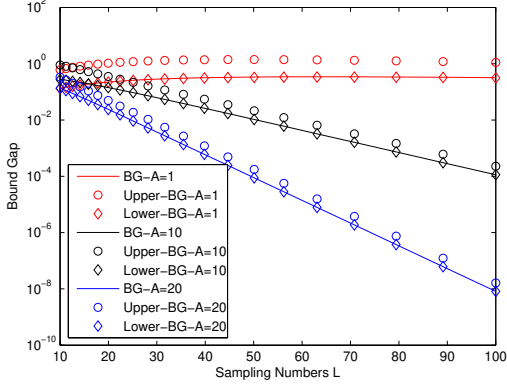


Fig. 5. The derived upper and lower bounds on $\Delta(\beta, \beta_1, \beta_2)$ versus sampling numbers L for different peak power.

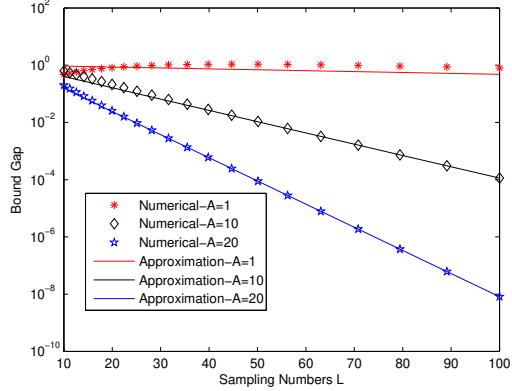


Fig. 6. The gap of derived upper and lower bounds on $\Delta(\beta, \beta_1, \beta_2)$ versus sampling numbers L from numerical computation and theoretical derivations for different peak power A .

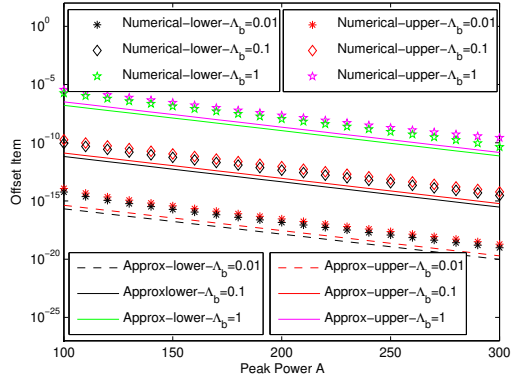
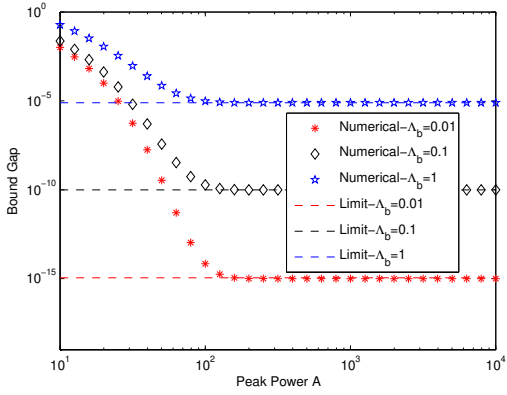


Fig. 7. The bound gap versus large peak power A from Fig. 8. The offset item $\epsilon_u + o(\epsilon_u)$ and $\epsilon_l + o(\epsilon_l)$ simulation and the limit for different background radiation versus large peak power A from numerical computation and exponential approximation for different background radiation arrival intensities Λ_0 .

bounds and the approximation are evaluated by the numerical results.

VIII. APPENDIX

A. Proof of Lemma 1

Note that $C_{1-\alpha}(P_0^B || P_1^B) = C_\alpha(P_1^B || P_0^B) \triangleq -L \ln f(\alpha)$, where $f(\alpha | p_0, p_1) = p_1^\alpha p_0^{1-\alpha} + (1 - p_1)^\alpha (1 - p_0)^{1-\alpha}$, we have

$$f'(\alpha | p_0, p_1) = p_0 \left(\frac{p_1}{p_0}\right)^\alpha \ln \frac{p_1}{p_0} + (1 - p_0) \left(\frac{1 - p_1}{1 - p_0}\right)^\alpha \ln \frac{1 - p_1}{1 - p_0}, \quad (51)$$

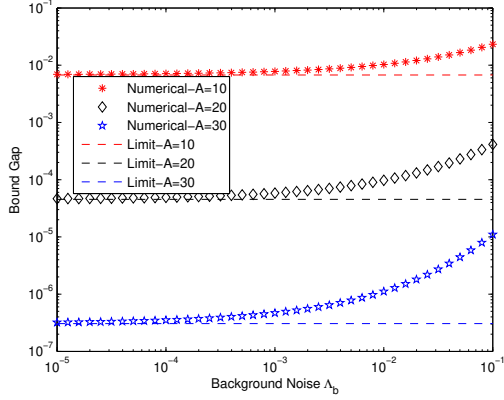


Fig. 9. The bound gap versus low background radiation arrival intensities Λ_0 from numerical computation and theoretical limit for different peak power A .

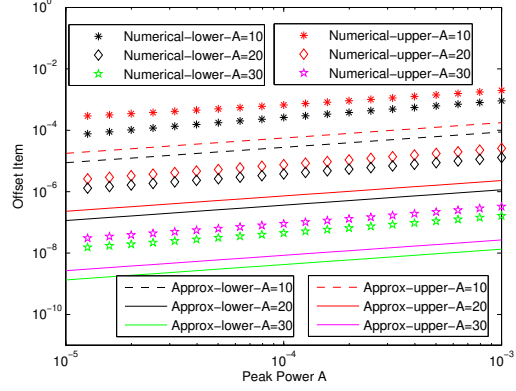


Fig. 10. The offset item $\epsilon'_u + o(\epsilon'_u)$ and $\epsilon'_l + o(\epsilon'_l)$ versus low background radiation arrival intensities Λ_0 from numerical computation and exponential approximation for different peak power A .

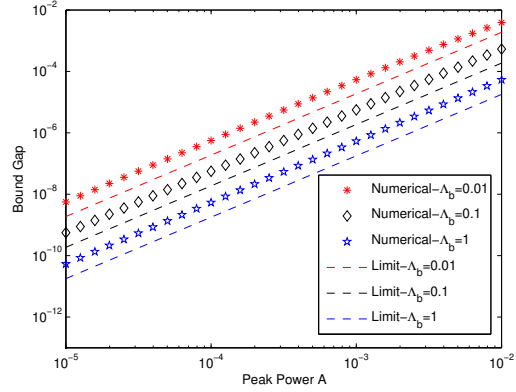
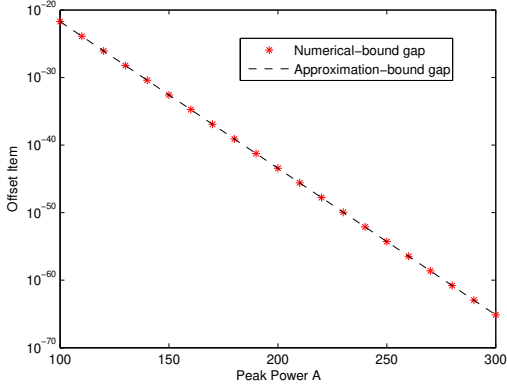


Fig. 11. The bound gap versus large peak power A from Fig. 12. The difference of derived upper and lower numerical computation and theoretical approximation for bounds on $\Delta(\beta, \beta_1, \beta_2)$ versus low peak power A from background radiation arrival intensities $\Lambda_0 = 0$.

and $f''(\alpha|p_0, p_1) > 0$, $f'(0|p_0, p_1) = -KL(p_0||p_1)$ and $f'(1|p_0, p_1) = KL(p_1||p_0) > 0$. Thus, the optimal α^Δ to maximize $C_\alpha(P_1^B||P_0^B)$ uniquely exists and satisfies $f'(\alpha^\Delta) = 0$, i.e.,

$$\alpha^\Delta(p_0, p_1) = \frac{\ln \frac{1-p_0}{p_0} + \ln \ln \frac{1-p_0}{1-p_1} - \ln \ln \frac{p_1}{p_0}}{\ln \frac{p_1(1-p_0)}{p_0(1-p_1)}}. \quad (52)$$

Since the symmetry $f(\alpha|p_0, p_1) = f(1 - \alpha|1 - p_1, 1 - p_0)$, we have $1 - \alpha^\Delta(p_0, p_1) = \alpha^\Delta(1 - p_1, 1 - p_0)$ and

$$\begin{aligned} \alpha^\Delta - (1 - \alpha^\Delta) &= \frac{[\ln \frac{1-p_0}{p_0} + \ln \ln \frac{1-p_0}{1-p_1} - \ln \ln \frac{p_1}{p_0}] - [\ln \frac{p_1}{1-p_1} + \ln \ln \frac{p_1}{p_0} - \ln \ln \frac{1-p_0}{1-p_1}]}{\ln \frac{p_1(1-p_0)}{p_0(1-p_1)}} \\ &= \frac{\ln \frac{(1-p_0)(1-p_1)}{p_0 p_1} + 2(\ln \ln \frac{1-p_0}{1-p_1} - \ln \ln \frac{p_1}{p_0})}{\ln \frac{p_1(1-p_0)}{p_0(1-p_1)}} \leq 0, \quad \text{if } p_0 + p_1 \geq 1, \end{aligned} \quad (53)$$

where the last inequality follows from the fact that the right term of the numerator of Equation (53) decreases with p_0 and becomes 0 for $p_0 = 1 - p_1$. Based on the above statement, we can readily obtain

$$\alpha^* = \arg \max_{0 \leq \alpha \leq 1} \min\{C_\alpha(P_1^B || P_0^B), C_{1-\alpha}(P_1^B || P_0^B)\} = \frac{1}{2}. \quad (54)$$

B. Proof of Lemma 2

Based on symmetry $F_u(\mu, \beta_1, \beta_2) = F_u(1 - \mu, \beta_2, \beta_1)$, we have

$$\frac{\partial F_u(\cdot, \beta_1, \beta_2)}{\partial \mu} \Big|_{\mu^*(\beta_1, \beta_2)} = -\frac{\partial F_u(\cdot, \beta_2, \beta_1)}{\partial \mu} \Big|_{1-\mu^*(\beta_2, \beta_1)} = 0, \quad (55)$$

i.e., $\mu^*(\beta_1, \beta_2) + \mu^*(\beta_2, \beta_1) = 1$. Defining $G(x, \beta) = \ln x - \frac{\beta}{x}$, we have

$$\begin{aligned} \frac{\partial F_u}{\partial \mu} \Big|_{(\mu^*(\beta_1, \beta_2), \beta_1, \beta_2)} &= G(1 - (1 - \beta_2)\mu, \frac{\beta_1 + \beta_2}{2}) - G(\beta_1 + (1 - \beta_1)\mu, \frac{\beta_1 + \beta_2}{2}) \\ &\quad + \frac{\beta_1 - \beta_2}{2} \left\{ \frac{1}{1 - (1 - \beta_2)\mu} + \frac{1}{\beta_1 + (1 - \beta_1)\mu} \right\} = 0. \end{aligned} \quad (56)$$

Thus we have $G(1 - (1 - \beta_2)\mu, \frac{\beta_1 + \beta_2}{2}) - G(\beta_1 + (1 - \beta_1)\mu, \frac{\beta_1 + \beta_2}{2}) \leq 0$ if $\beta_1 \geq \beta_2$. As $G(x, \beta)$ decreases with x , we can obtain $\mu^*(\beta_1, \beta_2) \geq \frac{1-\beta_1}{2-\beta_1-\beta_2}$ if $\beta_1 \geq \beta_2$.

C. Proof of Lemma 3

Consider the following three cases.

Case 1: $\beta_1 = \beta_2$. According to Equation (12), we have $\max_{0 \leq \mu \leq 1} F_u(\mu, \beta_1, \beta_2) = -\ln \frac{1+\beta_2}{2}$, i.e., the equality holds.

Case 2: $\beta_1 < \beta_2$. According to Lemma 2, we have

$$\ln \frac{\beta_1 + (1 - \beta_1)\mu^*(\beta_1, \beta_2)}{1 - (1 - \beta_2)\mu^*(\beta_1, \beta_2)} = \frac{\beta_1}{\beta_1 + (1 - \beta_1)\mu^*(\beta_1, \beta_2)} - \frac{\beta_2}{1 - (1 - \beta_2)\mu^*(\beta_1, \beta_2)} < 0. \quad (57)$$

As $\mu^*(\beta_1, \beta_2) < \frac{1-\beta_1}{2-\beta_1-\beta_2}$, we have the following upper bound on $\max_{0 \leq \mu \leq 1} F_u(\mu, \beta_1, \beta_2)$,

$$\begin{aligned}
F_u(\mu^*(\beta_1, \beta_2), \beta_1, \beta_2) &= -\ln[1 - (1 - \beta_2)\mu^*(\beta_1, \beta_2)] - \mu^*(\beta_1, \beta_2) \\
&\quad \cdot \left\{ \frac{\beta_1}{\beta_1 + (1 - \beta_1)\mu^*(\beta_1, \beta_2)} - \frac{\beta_2}{1 - (1 - \beta_2)\mu^*(\beta_1, \beta_2)} \right\} \\
&< -\ln \frac{1 - \beta_1\beta_2}{2 - \beta_1 - \beta_2} - \frac{\beta_1 - \beta_2}{(1 - \beta_1\beta_2)/(2 - \beta_1 - \beta_2)} \mu^*(\beta_1, \beta_2) \\
&< -\ln \frac{1 - \beta_1\beta_2}{2 - \beta_1 - \beta_2} + \frac{(\beta_2 - \beta_1)(1 - \beta_1)}{(1 - \beta_1\beta_2)}. \tag{58}
\end{aligned}$$

Case 3: $\beta_1 > \beta_2$. Similarly to Case 2, we have

$$F_u(\mu^*(\beta_1, \beta_2), \beta_1, \beta_2) < -\ln \frac{1 - \beta_1\beta_2}{2 - \beta_1 - \beta_2} + \frac{(\beta_1 - \beta_2)(1 - \beta_2)}{(1 - \beta_1\beta_2)}. \tag{59}$$

D. Proof of Theorem 2

Note that β , β_1 and β_2 approach 0 as L approaches infinity. According to Equation (15) and Taylor expansion $\ln(a + x) = \ln a + \frac{1}{a}x + o(x)$, we have

$$I_{max}(\Lambda_0, A, L) \geq -\ln \frac{1 + \beta}{2} = \ln 2 - \beta + o(\beta). \tag{60}$$

For $\beta_1 > \beta_2$, since $\frac{1-\beta_1\beta_2}{2-\beta_1-\beta_2} - \frac{1}{2} = \frac{\beta_1+\beta_2-2\beta_1\beta_2}{2(2-\beta_1-\beta_2)} = \frac{\beta_1}{4} + o(\beta_1)$, we have

$$\begin{aligned}
I_{max}(\Lambda_0, A, L) &\leq \frac{|\beta_1 - \beta_2|(1 - \min\{\beta_1, \beta_2\})}{1 - \beta_1\beta_2} - \ln \frac{1 - \beta_1\beta_2}{2 - \beta_1 - \beta_2} \\
&= \beta_1 + o(\beta_1) + \ln 2 - \frac{\beta_1}{2} + o(\beta_1) = \ln 2 + \frac{\beta_1}{2} + o(\beta_1). \tag{61}
\end{aligned}$$

Similarly, for $\beta_1 < \beta_2$, we have $I_{max}(\Lambda_0, A, L) \leq \ln 2 + \frac{\beta_2}{2} + o(\beta_2)$. Thus, $I_{max}(\Lambda_0, A, L) \leq \ln 2 + \frac{\max\{\beta_1, \beta_2\}}{2} + o(\max\{\beta_1, \beta_2\})$ for $\beta_1 \neq \beta_2$.

For For $\beta_1 = \beta_2$, we have

$$\begin{aligned}
I_{max}(\Lambda_0, A, L) &= \frac{|\beta_1 - \beta_2|(1 - \min\{\beta_1, \beta_2\})}{1 - \beta_1\beta_2} - \ln \frac{1 - \beta_1\beta_2}{2 - \beta_1 - \beta_2} \\
&= -\ln \frac{1 + \beta_1}{2} = \ln 2 - \beta_1 + o(\beta_1). \tag{62}
\end{aligned}$$

E. Proof of Lemma 4

As $\beta = (\sqrt{p_0 p_1} + \sqrt{(1-p_0)(1-p_1)})^L$ and $1 - \sqrt{x} = \frac{1}{2}(1-x) + o(1-x)$ for $x \rightarrow 1$, we have

$$\begin{aligned}
& p_0^{\frac{L}{2}} - (\sqrt{p_0 p_1} + \sqrt{(1-p_0)(1-p_1)})^L \\
&= (\sqrt{p_0} - \sqrt{p_0 p_1} - \sqrt{(1-p_0)(1-p_1)}) \sum_{i=0}^{L-1} (p_0^{\frac{L}{2}})^i (\sqrt{p_0 p_1} + \sqrt{(1-p_0)(1-p_1)})^{L-1-i} \\
&= p_0^{\frac{L-1}{2}} \left(\frac{\sqrt{p_0}}{2} (1-p_1) - \sqrt{(1-p_0)(1-p_1)}^{\frac{1}{2}} \right) + o(1-p_1). \tag{63}
\end{aligned}$$

Since $\beta_1 = \left(\frac{p_0}{p_1}\right)^{p_1 L} \left(\frac{1-p_0}{1-p_1}\right)^{(1-p_1)L}$ and $1 - x^{-ax} = ax \ln x + o(x \ln x) = -a(1-x) + o(1-x)$ for $x \rightarrow 1$, we have

$$\begin{aligned}
p_0^L - \beta_1 &= p_0^L \left(1 - \left(\frac{1}{p_1}\right)^{p_1 L} \left(\frac{1-p_0}{1-p_1}\right)^{(1-p_1)L} \right) \\
&= p_0^L \left(\left(1 - \left(\frac{1}{p_1}\right)^{p_1 L}\right) + \left(\frac{1}{p_1}\right)^{p_1 L} \left(1 - \left(\frac{1-p_0}{1-p_1}\right)^{(1-p_1)L}\right) \right) \\
&= p_0^L \left(-L(1-p_1) + (1-p_1)L \ln \frac{1-p_1}{1-p_0} \right) + o(1-p_1). \tag{64}
\end{aligned}$$

Noting that $\beta_2 = \left(\frac{p_1}{p_0}\right)^{p_0 L} \left(\frac{1-p_1}{1-p_0}\right)^{(1-p_0)L}$, we have

$$\begin{aligned}
& \left(\frac{1}{p_0}\right)^{p_0 L} \left(\frac{1}{1-p_0}\right)^{(1-p_0)L} (1-p_1)^{(1-p_0)L} - \beta_2 \\
&= \left(\frac{1}{p_0}\right)^{p_0 L} \left(\frac{1}{1-p_0}\right)^{(1-p_0)L} (1-p_1)^{(1-p_0)L} (1-p_1^{L p_0}) \\
&= \left(\frac{1}{p_0}\right)^{p_0 L} \left(\frac{1}{1-p_0}\right)^{(1-p_0)L} (1-p_1)^{(1-p_0)L} L p_0 (1-p_1) + o(1-p_1) = o(1-p_1). \tag{65}
\end{aligned}$$

F. Proof of Theorem 3

For large A , p_1 and β_2 approach 1 and 0, respectively. According to Lemma 4, Equation (15) and $\ln(a+x) = \ln a + \frac{x}{a} + o(x)$, we have

$$\begin{aligned}
I_{max}(\Lambda_0, A, L) &\geq -\ln \frac{1+\beta}{2} \\
&= \ln \frac{2}{1+p_0^{\frac{L}{2}}} + \frac{p_0^{\frac{L-1}{2}}}{1+p_0^{\frac{L}{2}}} \left(\frac{\sqrt{p_0}}{2} (1-p_1) - \sqrt{(1-p_0)(1-p_1)}^{\frac{1}{2}} \right) + o(1-p_1). \tag{66}
\end{aligned}$$

For the upper bound, since

$$\frac{1 - \beta_1 \beta_2}{2 - \beta_1 - \beta_2} - \frac{1}{2 - \beta_1} = \frac{-(1 + 2\beta_1 - \beta_1^2)\beta_2}{(2 - \beta_1 - \beta_2)(2 - \beta_1)} = \frac{-(1 + 2\beta_1 - \beta_1^2)\beta_2}{(2 - \beta_1)^2} + o(\beta_2), \tag{67}$$

the maximal mutual information is given by

$$\begin{aligned}
I_{max}(\Lambda_0, A, L) &\leq \frac{|\beta_1 - \beta_2|(1 - \min\{\beta_1, \beta_2\})}{1 - \beta_1\beta_2} - \ln \frac{1 - \beta_1\beta_2}{2 - \beta_1 - \beta_2} \\
&= \beta_1 - (1 + \beta_1)\beta_2 + o(\beta_2) + \ln(2 - \beta_1) + \frac{-(1 + 2\beta_1 - \beta_1^2)\beta_2}{2 - \beta_1} + o(\beta_2) \\
&= p_0^L + \ln(2 - p_0^L) + O(\max\{(1 - p_1) \ln(1 - p_1), (1 - p_1)^{(1-p_0)L}\}). \quad (68)
\end{aligned}$$

G. Proof of Theorem 4

Note that $\frac{\partial F_u}{\partial \beta_1} = -\frac{\mu(1-\mu)}{(1-\mu)\beta_1 + \mu} < 0$, $\frac{\partial F_u}{\partial \beta_2} = -\frac{\mu(1-\mu)}{\mu\beta_2 + 1 - \mu} < 0$, $\frac{\partial^2 F_u}{\partial \beta_1^2} = \frac{\mu(1-\mu)^2}{[(1-\mu)\beta_1 + \mu]^2} > 0$ and $\frac{\partial^2 F_u}{\partial \beta_2^2} = \frac{\mu^2(1-\mu)}{[\mu\beta_2 + 1 - \mu]^2} > 0$. **For low SNR**, according to Taylor Theorem and $\beta > \max\{\beta_1, \beta_2\}$, we have

$$\begin{aligned}
F_u(\mu, \beta_1, \beta_2) - F_u(\mu, \beta, \beta_2) &\stackrel{(a)}{=} \frac{\mu(1-\mu)}{(1-\mu)\beta_1 + \mu}(\beta - \beta_1) + \frac{\partial^2 F_u}{\partial \beta_1^2} \Big|_{(\beta, \xi_1, \beta_2)} (\beta - \beta_1)^2 \\
&\stackrel{(b)}{\leq} \frac{\mu(1-\mu)}{(1-\mu)\beta_1 + \mu}(\beta - \beta_1) + \frac{\partial^2 F_u}{\partial \beta_1^2} \Big|_{(\beta, \beta_1, \beta_2)} (\beta - \beta_1)^2, \quad (69)
\end{aligned}$$

where (a) holds due to the Taylor expansion in terms of β_1 , $\xi_1 \in (\beta_1, \beta)$ and (b) holds since $\frac{\partial^2 F_u}{\partial \beta_1^2}$ is monotone decreasing with respect to β_1 . Furthermore, we have

$$\begin{aligned}
\max_{\mu \in [0,1]} F_u(\mu, \beta_1, \beta_2) - F_u(\mu, \beta, \beta_2) &\leq \max_{\mu \in [0,1]} \frac{\mu(1-\mu)}{(1-\mu)\beta_1 + \mu}(\beta - \beta_1) + \frac{\mu(1-\mu)^2}{[(1-\mu)\beta_1 + \mu]^2}(\beta - \beta_1)^2 \\
&\stackrel{(c)}{\leq} \frac{1}{4\beta_1}(\beta - \beta_1) + \frac{4}{27\beta_1^2}(\beta - \beta_1)^2, \quad (70)
\end{aligned}$$

where (c) holds since $(1-\mu)\beta_1 + \mu \geq \beta_1$, $\mu(1-\mu) \leq (\frac{\mu+(1-\mu)}{2})^2 = \frac{1}{4}$ and $\mu(1-\mu)^2 \leq \frac{1}{2}(\frac{2\mu+(1-\mu)+(1-\mu)}{3})^2 = \frac{4}{27}$. Similar to equation (70), we have

$$\max_{\mu \in [0,1]} F_u(\mu, \beta, \beta_2) - F_u(\mu, \beta, \beta) \leq \frac{1}{4\beta_2}(\beta - \beta_2) + \frac{4}{27\beta_2^2}(\beta - \beta_2)^2. \quad (71)$$

As $F_l(\mu, \beta) = F_u(\mu, \beta, \beta)$, we have the upper bound on $\Delta(\beta, \beta_1, \beta_2)$ in low SNR regime,

$$\begin{aligned}
\Delta(\beta, \beta_1, \beta_2) &= \max_{\mu \in [0,1]} F_u(\mu, \beta_1, \beta_2) - F_u(\mu, \beta, \beta) \\
&\stackrel{(d)}{\leq} \max_{\mu \in [0,1]} F_u(\mu, \beta_1, \beta_2) - F_u(\mu, \beta, \beta_2) + \max_{\mu \in [0,1]} F_u(\mu, \beta, \beta_2) - F_u(\mu, \beta, \beta) \\
&\stackrel{(e)}{\leq} \frac{1}{4\beta_1}(\beta - \beta_1) + \frac{4}{27\beta_1^2}(\beta - \beta_1)^2 + \frac{1}{4\beta_2}(\beta - \beta_2) + \frac{4}{27\beta_2^2}(\beta - \beta_2)^2 \\
&= \frac{1}{108}(\frac{\beta}{\beta_1} - 1)(16\frac{\beta}{\beta_1} + 11) + \frac{1}{108}(\frac{\beta}{\beta_2} - 1)(16\frac{\beta}{\beta_2} + 11), \quad (72)
\end{aligned}$$

where (d) holds due to $\max_x f(x) + g(x) \leq \max_x f(x) + \max_x g(x)$ and (e) holds according to Equations (70) and (71).

For high SNR, note that

$$\begin{aligned} F_u(\mu, \beta_1, \beta_2) - F_u(\mu, \beta, \beta_2) &= \mu \ln \left[1 + \frac{(1-\mu)(\beta-\beta_1)}{(1-\mu)\beta_1 + \mu} \right] \stackrel{(f)}{\leq} \frac{\mu(1-\mu)(\beta-\beta_1)}{(1-\mu)\beta_1 + \mu} \\ &\stackrel{(g)}{\leq} (1-\mu)(\beta-\beta_1), \end{aligned} \quad (73)$$

where (f) and (g) hold due to $\ln(1+x) \leq x$ and $\mu \leq (1-\mu)\beta_1 + \mu$, respectively. Thus, we have

$$\max_{\mu \in [0,1]} F_u(\mu, \beta_1, \beta_2) - F_u(\mu, \beta, \beta_2) \leq \beta - \beta_1. \quad (74)$$

Similarly to Equation (74), we have

$$\max_{\mu \in [0,1]} F_u(\mu, \beta, \beta_2) - F_u(\mu, \beta, \beta) \leq \beta - \beta_2. \quad (75)$$

Thus, we have the following upper bound on $\Delta(\beta, \beta_1, \beta_2)$ in high SNR regime,

$$\begin{aligned} \Delta(\beta, \beta_1, \beta_2) &\leq \max_{\mu \in [0,1]} F_u(\mu, \beta_1, \beta_2) - F_u(\mu, \beta, \beta_2) + \max_{\mu \in [0,1]} F_u(\mu, \beta, \beta_2) - F_u(\mu, \beta, \beta) \\ &\leq (\beta - \beta_1) + (\beta - \beta_2). \end{aligned} \quad (76)$$

For general β, β_1, β_2 , we have the following lower bound on $\Delta(\beta, \beta_1, \beta_2)$,

$$\begin{aligned} \Delta(\beta, \beta_1, \beta_2) &= \max_{\mu \in [0,1]} F_u(\beta, \beta_1, \beta_2) - F_u(\beta, \beta, \beta) \\ &\stackrel{(g)}{\geq} \max_{\mu \in [0,1]} F_u(\beta, \beta_1, \beta_2) - \max_{\mu \in [0,1]} F_u(\beta, \beta, \beta) \\ &= \max_{\mu \in [0,1]} F_u(\beta, \beta_1, \beta_2) + \ln \frac{1+\beta}{2} \\ &\stackrel{\mu=\frac{1}{2}}{\geq} -\frac{1}{2} \left(\ln \frac{1+\beta_1}{2} + \ln \frac{1+\beta_2}{2} \right) + \ln \frac{1+\beta}{2} = \frac{1}{2} \ln \frac{1+\beta}{1+\beta_1} + \frac{1}{2} \ln \frac{1+\beta}{1+\beta_2}, \end{aligned}$$

where (g) holds since that for positive function $f(x)$ and $g(x)$,

$$\max_x f(x) - g(x) \geq f(x^*) - g(x^*) \geq f(x^*) - \max_x g(x) = \max_x f(x) - \max_x g(x),$$

and $x^* = \arg \max_x f(x)$.

H. Proof of Theorem 5

As $\beta = \exp(-C_{\frac{1}{2}}(P_1^B||P_0^B)) \rightarrow 0$, $\beta_1 = \exp(-KL(P_1^B||P_0^B)) \rightarrow 0$ and $\beta_2 = \exp(-KL(P_0^B||P_1^B)) \rightarrow 0$ as L approaches infinity, such scenario corresponds to high SNR regime. According to Theorem 4, $\beta_1 = o(\beta)$ and $\beta_2 = o(\beta)$, we have

$$\begin{aligned} \Delta(\beta, \beta_1, \beta_2) &\leq (\beta - \beta_1) + (\beta - \beta_2) \\ &= 2 \exp(-C_{\frac{1}{2}}(P_1^B||P_0^B)) + o(\exp(-C_{\frac{1}{2}}(P_1^B||P_0^B))). \end{aligned} \quad (77)$$

Thus, we have the following lower bound on the exponential rate of $\Delta(\beta, \beta_1, \beta_2)$ with respect to L ,

$$-\lim_{L \rightarrow \infty} \frac{\ln \Delta(\beta, \beta_1, \beta_2)}{L} \geq \lim_{L \rightarrow \infty} \frac{C_{\frac{1}{2}}(P_1^B||P_0^B)}{L} = -\ln(\sqrt{p_0 p_1} + \sqrt{(1-p_0)(1-p_1)}). \quad (78)$$

Similarly, we have

$$\Delta(\beta, \beta_1, \beta_2) \geq \frac{1}{2} \ln \frac{1+\beta}{1+\beta_1} + \frac{1}{2} \ln \frac{1+\beta}{1+\beta_2} = \frac{1}{2} \frac{\beta - \beta_1}{1+\beta_1} + \frac{1}{2} \frac{\beta - \beta_2}{1+\beta_2} + o(\beta) = \beta + o(\beta); \quad (79)$$

and thus an upper bound on exponential rate of $\Delta(\beta, \beta_1, \beta_2)$ with respect to L is given as follows,

$$-\lim_{L \rightarrow \infty} \frac{\ln \Delta(\beta, \beta_1, \beta_2)}{L} \leq \lim_{L \rightarrow \infty} \frac{C_{\frac{1}{2}}(P_1^B||P_0^B)}{L} = -\ln(\sqrt{p_0 p_1} + \sqrt{(1-p_0)(1-p_1)}). \quad (80)$$

From Equations (78) and (80), we have

$$-\lim_{L \rightarrow \infty} \frac{\ln \Delta(\beta, \beta_1, \beta_2)}{L} = -\ln(\sqrt{p_0 p_1} + \sqrt{(1-p_0)(1-p_1)}). \quad (81)$$

It demonstrates the asymptotic tightness of the upper and lower bounds for large L , with exponential rate $-\ln(\sqrt{p_0 p_1} + \sqrt{(1-p_0)(1-p_1)})$.

I. Proof of Theorem 6

According to Lemma 4 and Theorem 4, we have the upper bound on $\Delta(\beta, \beta_1, \beta_2)$,

$$\Delta(\beta, \beta_1, \beta_2) \leq (\beta - \beta_1) + (\beta - \beta_2) = 2p_0^{\frac{L}{2}} - p_0^L + \epsilon_u + o(\epsilon_u), \quad (82)$$

where ϵ_u is shown in Equation (36). Similarly, according to Theorem 4, we have the following upper bound on $\Delta(\beta, \beta_1, \beta_2)$,

$$\Delta(\beta, \beta_1, \beta_2) \geq \ln(1 + p_0^{\frac{L}{2}}) - \frac{1}{2} \ln(1 + p_0^L) + \epsilon_l + o(\epsilon_l), \quad (83)$$

where ϵ_l is showed in equation (37).

J. Proof of Theorem 8

According to Theorem 4, we have the following upper and lower bounds on bound gap $\Delta(\beta, \beta_1, \beta_2)$,

$$\begin{aligned}\Delta(\beta, \beta_1, \beta_2) &\leq (\beta - \beta_1) + (\beta - \beta_2), \\ &= 2(1 - p_1)^{\frac{L}{2}} + o((1 - p_1)^{\frac{L}{2}}),\end{aligned}\tag{84}$$

$$\begin{aligned}\Delta(\beta, \beta_1, \beta_2) &\geq \frac{1}{2} \ln \frac{1 + \beta}{1 + \beta_1} + \frac{1}{2} \ln \frac{1 + \beta}{1 + \beta_2} \\ &= \frac{1}{2}(1 - p_1)^{\frac{L}{2}} + \frac{1}{2} \frac{(1 - p_1)^{\frac{L}{2}} - (1 - p_1)^L}{1 + (1 - p_1)^L} + o((1 - p_1)^{\frac{L}{2}}) \\ &= (1 - p_1)^{\frac{L}{2}} + o((1 - p_1)^{\frac{L}{2}}).\end{aligned}\tag{85}$$

Thus, the asymptotic tightness is demonstrated as follows,

$$\begin{aligned}0 = \lim_{A \rightarrow \infty} (1 - p_1)^{\frac{L}{2}} + o((1 - p_1)^{\frac{L}{2}}) &\leq \lim_{A \rightarrow \infty} \Delta(\beta, \beta_1, \beta_2) \\ &\leq \lim_{A \rightarrow \infty} 2(1 - p_1)^{\frac{L}{2}} + o((1 - p_1)^{\frac{L}{2}}) = 0.\end{aligned}\tag{86}$$

Furthermore, we have the following on the exponential rate of the bound gap with respect to peak power A ,

$$-\lim_{A \rightarrow \infty} \frac{\ln \Delta(\beta, \beta_1, \beta_2)}{A} \geq \lim_{A \rightarrow \infty} -\frac{\ln[2(1 - p_1)^{\frac{L}{2}} + o((1 - p_1)^{\frac{L}{2}})]}{A} = \frac{L\tau}{2},\tag{87}$$

$$-\lim_{A \rightarrow \infty} \frac{\ln \Delta(\beta, \beta_1, \beta_2)}{A} \leq \lim_{A \rightarrow \infty} -\frac{\ln[(1 - p_1)^{\frac{L}{2}} + o((1 - p_1)^{\frac{L}{2}})]}{A} = \frac{L\tau}{2},\tag{88}$$

i.e., $-\lim_{A \rightarrow \infty} \frac{\ln \Delta(\beta, \beta_1, \beta_2)}{A} = \frac{L\tau}{2}$.

K. Proof of Theorem 9

For low peak power A , we have $p_1 \rightarrow p_0$ and $p_1 - p_0 = e^{-\Lambda_0 \tau}(1 - e^{-A\tau}) = (1 - p_0)\tau A + o(A)$.

Noting that $\sqrt{x + p_0} = \sqrt{p_0} + \frac{1}{2\sqrt{p_0}}x - \frac{1}{8p_0^{\frac{3}{2}}}x^2 + o(x^2)$, we have

$$\begin{aligned}&1 - \sqrt{p_0 p_1} - \sqrt{(1 - p_0)(1 - p_1)} \\ &= 1 - \left(p_0 + \frac{p_1 - p_0}{2} - \frac{(p_1 - p_0)^2}{8p_0}\right) - \left(1 - p_0 + \frac{p_0 - p_1}{2} - \frac{(p_0 - p_1)^2}{8(2 - p_0)}\right) + o(A^2) \\ &= \frac{(p_1 - p_0)^2}{8p_0(1 - p_0)} + o(A^2) = \frac{(1 - p_0)}{8p_0} \tau^2 A^2 + o(A^2).\end{aligned}\tag{89}$$

Thus, we have the following Taylor expansion on β ,

$$\begin{aligned}
\beta &= \exp(-C_{\frac{1}{2}}(P_1^B||P_0^B)) = 1 - C_{\frac{1}{2}}(P_1^B||P_0^B) + o(C_{\frac{1}{2}}(P_1^B||P_0^B)) \\
&= 1 - L(1 - \sqrt{p_0 p_1} - \sqrt{(1-p_0)(1-p_1)}) + o(1 - \sqrt{p_0 p_1} - \sqrt{(1-p_0)(1-p_1)}) \\
&= 1 - \frac{L(1-p_0)}{8p_0} \tau^2 A^2 + o(A^2).
\end{aligned} \tag{90}$$

Note that $KL(P_1^B||P_0^B) = L(p_1 \ln \frac{p_1}{p_0} + (1-p_1) \ln \frac{1-p_1}{1-p_0})$, according to Taylor theorem, we have

$$\begin{aligned}
KL(P_1^B||P_0^B) &= 0 + L\left(\ln \frac{p_1}{p_0} - \ln \frac{1-p_1}{1-p_0}\right)\Big|_{p_1=p_0} (p_1 - p_0) \\
&\quad + \frac{L}{p_1(1-p_1)}\Big|_{p_1=p_0} \frac{(p_1 - p_0)^2}{2} + o((p_1 - p_0)^2) \\
&= \frac{L(1-p_0)}{2p_0} \tau^2 A^2 + o(A^2).
\end{aligned} \tag{91}$$

Thus, we have the following Taylor expansion on the β_1 ,

$$\begin{aligned}
\beta_1 &= \exp(-KL(P_1^B||P_0^B)) = 1 - KL(P_1^B||P_0^B) + o(KL(P_1^B||P_0^B)) \\
&= 1 - \frac{L(1-p_0)}{2p_0} \tau^2 A^2 + o(A^2).
\end{aligned} \tag{92}$$

Similarly, we have the following Taylor expansion on the β_2 ,

$$\beta_2 = 1 - \frac{L(1-p_0)}{2p_0} \tau^2 A^2 + o(A^2). \tag{93}$$

According to Theorem 4, we have

$$\begin{aligned}
\Delta(\beta, \beta_1, \beta_2) &\leq \frac{1}{108} \left(\frac{\beta}{\beta_1} - 1\right) \left(16 \frac{\beta}{\beta_1} + 11\right) + \frac{1}{108} \left(\frac{\beta}{\beta_2} - 1\right) \left(16 \frac{\beta}{\beta_2} + 11\right) \\
&= \frac{1}{108} \left(\frac{L(1-p_0)}{2p_0} - \frac{L(1-p_0)}{8p_0}\right) \tau^2 A^2 \times 27 \times 2 + o(A^2) \\
&= \frac{3L(1-p_0)}{16p_0} \tau^2 A^2 + o(A^2),
\end{aligned} \tag{94}$$

$$\Delta(\beta, \beta_1, \beta_2) \geq \frac{1}{2} \ln \frac{1+\beta}{1+\beta_1} + \frac{1}{2} \ln \frac{1+\beta}{1+\beta_2} = \frac{3L(1-p_0)}{16p_0} \tau^2 A^2 + o(A^2). \tag{95}$$

Based on Equations (94) and (95), we have $\Delta(\beta, \beta_1, \beta_2) = \frac{3L(1-p_0)}{16p_0} \tau^2 A^2 + o(A^2)$.

L. Proof of Theorem 10

Note that for binomial distribution P_i^B , we have the following approximation on entropy [35, Theorem 2],

$$H(P_i^B) = \frac{1}{2} \ln 2\pi e L p_i (1 - p_i) + O\left(\frac{1}{L}\right), i = 0, 1. \quad (96)$$

Since $\mathbb{P}(\hat{N} = 0 | X = 0) = (1 - p_0)^L = 1 - Lp_0 + o(Lp_0)$, defining random variable $\hat{Y} \sim \mathbb{B}(1, Lp_0)$, we have $H(P_0^B) - H(\hat{Y}) = o(Lp_0)$ and

$$H(\hat{N} | X) = \frac{\mu}{2} \ln[2\pi e L p_1 (1 - p_1)] + (1 - \mu) h_b(Lp_0) + O\left(\frac{1}{L}\right) + o(Lp_0). \quad (97)$$

Considering the mixture distribution of \hat{N} , we have

$$\mathbb{P}(\hat{N} = 0) = \mu(1 - p_1)^L + (1 - \mu)(1 - Lp_0) + o(Lp_0) \triangleq q_0 + o(Lp_0); \quad (98)$$

$$\mathbb{P}(\hat{N} = 1) = \mu L p_1 (1 - p_1)^{L-1} + (1 - \mu)Lp_0 + o(Lp_0) \triangleq q_1 + o(Lp_0); \quad (99)$$

$$\mathbb{P}(\hat{N} = i) = \mu \binom{L}{i} p_1^i (1 - p_1)^{L-i} + o(Lp_0) \triangleq q_i + o(Lp_0), \text{ for } i \geq 2. \quad (100)$$

According to the continuity of entropy function, we have

$$H(\hat{N}) = - \sum_{i=0}^L q_i \ln q_i + o(Lp_0). \quad (101)$$

Based on Taylor expansion, we have

$$\begin{aligned} -q_0 \ln q_0 &= -[\mu(1 - p_1)^L + 1 - \mu] \ln[\mu(1 - p_1)^L + 1 - \mu] \\ &\quad + (1 - \mu)Lp_0 \{1 + \ln[\mu(1 - p_1)^L + 1 - \mu]\} + o(Lp_0), \end{aligned} \quad (102)$$

$$\begin{aligned} -q_1 \ln q_1 &= -\mu L p_1 (1 - p_1)^{L-1} [\ln(\mu L p_1) + (L - 1) \ln(1 - p_1)] \\ &\quad - (1 - \mu)Lp_0 [1 + \ln(\mu L p_1) + (L - 1) \ln(1 - p_1)] + o(Lp_0), \end{aligned} \quad (103)$$

$$\begin{aligned} - \sum_{i=2}^L q_i \ln q_i &= -\mu \ln \mu [1 - q_0 - q_1] + \mu H(P_1^B) + \mu \left\{ L(1 - p_1)^L \ln(1 - p_1) \right. \\ &\quad \left. + L p_1 (1 - p_1)^{L-1} [\ln(L p_1) + (L - 1) \ln(1 - p_1)] \right\}. \end{aligned} \quad (104)$$

Since $I(X; \hat{N}) = H(\hat{N}) - H(\hat{N} | X)$, we can obtain Equation (50).

REFERENCES

- [1] Z. Xu and B. M. Sadler, "Ultraviolet communications: potential and state-of-the-art," *IEEE Communications Magazine*, vol. 46, no. 5, May. 2008.
- [2] H. Ding, G. Chen, A. K. Majumdar, B. M. Sadler, and Z. Xu, "Modeling of non-line-of-sight ultraviolet scattering channels for communication," *IEEE Journal on Selected Areas in Communications*, vol. 27, no. 9, Sept. 2009.
- [3] H. Zhang, H. Yin, H. Jia, S. Chang, and J. Yang, "Characteristics of non-line-of-sight polarization ultraviolet communication channels," *Applied Optics*, vol. 51, no. 35, pp. 8366–8372, 2012.
- [4] A. Gupta, M. Noshad, and M. Brandt-Pearce, "Nlos uv channel modeling using numerical integration and an approximate closed-form path loss model," in *Laser Communication and Propagation through the Atmosphere and Oceans*, vol. 8517. International Society for Optics and Photonics, 2012, p. 851709.
- [5] Y. Zuo, H. Xiao, J. Wu, W. Li, and J. Lin, "Closed-form path loss model of non-line-of-sight ultraviolet single-scatter propagation," *Optics Letters*, vol. 38, no. 12, pp. 2116–2118, 2013.
- [6] Y. Sun and Y. Zhan, "Closed-form impulse response model of non-line-of-sight single-scatter propagation," *JOSA A*, vol. 33, no. 4, pp. 752–757, 2016.
- [7] G. Chen, L. Liao, Z. Li, R. J. Drost, and B. M. Sadler, "Experimental and simulated evaluation of long distance nlos uv communication," in *Communication Systems, Networks & Digital Signal Processing (CSNDSP), 2014 9th International Symposium on*. IEEE, 2014, pp. 904–909.
- [8] L. Liao, Z. Li, T. Lang, and G. Chen, "Uv led array based nlos uv turbulence channel modeling and experimental verification," *Optics express*, vol. 23, no. 17, pp. 21 825–21 835, 2015.
- [9] N. Raptis, E. Pikasis, and D. Syvridis, "Power losses in diffuse ultraviolet optical communications channels," *Optics letters*, vol. 41, no. 18, pp. 4421–4424, 2016.
- [10] A. D. Wyner, "Capacity and error exponent for the direct detection photon channel-part I-II," *IEEE Transactions on Information Theory*, vol. 34, no. 6, pp. 1449–1471, Jun. 1988.
- [11] M. R. Frey, "Information capacity of the poisson channel," *IEEE Transactions on Information Theory*, vol. 37, no. 2, pp. 244–256, Feb. 1991.
- [12] A. Lapidoth and S. M. Moser, "On the capacity of the discrete-time poisson channel," *IEEE Transactions on Information Theory*, vol. 55, no. 1, pp. 303–322, Jan. 2009.
- [13] J. Cao, S. Hranilovic, and J. Chen, "Capacity-achieving distributions for the discrete-time poisson channel part i: General properties and numerical techniques," *IEEE Transactions on Communications*, vol. 62, no. 1, pp. 194–202, Jan. 2014.
- [14] L. Lai, Y. Liang, and S. S. Shitz, "On the capacity bounds for poisson interference channels," *IEEE Transactions on Information Theory*, vol. 61, no. 1, pp. 223–238, Jan. 2015.
- [15] M. A. El-Shimy and S. Hranilovic, "Binary-input non-line-of-sight solar-blind uv channels: Modeling, capacity and coding," *IEEE/OSA Journal of Optical Communications and Networking*, vol. 4, no. 12, pp. 1008–1017, Dec. 2012.
- [16] Z. Jiang, C. Gong, and Z. Xu, "Clipping noise and power allocation for ofdm-based optical wireless communication using photon detection," *IEEE Wireless Communications Letters*, in press, 2018.
- [17] C. Gong and Z. Xu, "Non-line of sight optical wireless relaying with the photon counting receiver: A count-and-forward protocol," *IEEE Transactions on Wireless Communications*, vol. 14, no. 1, pp. 376–388, Jan. 2015.
- [18] M. H. Ardakani and M. Uysal, "Relay-assisted ofdm for ultraviolet communications: performance analysis and optimization," *IEEE Transactions on Wireless Communications*, vol. 16, no. 1, pp. 607–618, Jan. 2017.
- [19] M. H. Ardakani, A. R. Heidarpour, and M. Uysal, "Performance analysis of relay-assisted nlos ultraviolet communications over turbulence channels," *IEEE/OSA Journal of Optical Communications and Networking*, vol. 9, no. 1, pp. 109–118, Jan. 2017.

- [20] W. Becker, *Advanced time-correlated single photon counting techniques*. Springer Science & Business Media, 2005.
- [21] D. Chitnis and S. Collins, "A spad-based photon detecting system for optical communications," *IEEE Journal of Lightwave Technology*, vol. 32, no. 10, pp. 2028–2034, May. 2014.
- [22] S. Gnechchi, N. A. Dutton, L. Parmesan, B. R. Rae, S. Pellegrini, S. J. McLeod, L. A. Grant, and R. K. Henderson, "Analysis of photon detection efficiency and dynamic range in spad-based visible light receivers," *Journal of Lightwave Technology*, vol. 34, no. 11, pp. 2774–2781, 2016.
- [23] S. R. Cherry, J. A. Sorenson, and M. E. Phelps, *Physics in nuclear medicine e-Book*. Elsevier Health Sciences, 2012.
- [24] K. Omote, "Dead-time effects in photon counting distributions," *Nuclear Instruments and Methods in Physics Research Section A: Accelerators, Spectrometers, Detectors and Associated Equipment*, vol. 293, no. 3, pp. 582–588, 1990.
- [25] F. Y. Daniel and J. A. Fessler, "Mean and variance of single photon counting with deadtime," *Physics in Medicine & Biology*, vol. 45, no. 7, p. 2043, 2000.
- [26] R. J. Drost, B. M. Sadler, and G. Chen, "Dead time effects in non-line-of-sight ultraviolet communications," *Optics Express*, vol. 23, no. 12, pp. 15 748–15 761, 2015.
- [27] E. Sarbazi and H. Haas, "Detection statistics and error performance of spad-based optical receivers," in *Personal, Indoor, and Mobile Radio Communications (PIMRC), 2015 IEEE 26th Annual International Symposium on*, 2015, pp. 830–834.
- [28] E. Sarbazi, M. Safari, and H. Haas, "On the information transfer rate of spad receivers for optical wireless communications," in *Global Communications Conference (GLOBECOM), 2016 IEEE*. IEEE, 2016, pp. 1–6.
- [29] E. Sarbazi, M. Safari, and H. Hass, "Statistical modeling of single-photon avalanche diode receivers for optical wireless communications," *IEEE Transactions on Communications*, vol. 66, no. 9, pp. 4043–4058, Sep. 2018.
- [30] G.-L. Shentu, Q.-C. Sun, X. Jiang, X.-D. Wang, J. S. Pelc, M. Fejer, Q. Zhang, and J.-W. Pan, "217 km long distance photon-counting optical time-domain reflectometry based on ultra-low noise up-conversion single photon detector," *Optics Express*, vol. 21, no. 21, pp. 24 674–24 679, 2013.
- [31] D. Zou, C. Gong, K. Wang, and Z. Xu, "Characterization on practical photon counting receiver in optical scattering communication," *IEEE Transactions on Communications*, in press, 2018.
- [32] A. Kolchinsky and B. D. Tracey, "Estimating mixture entropy with pairwise distances," *Entropy*, vol. 19, no. 7, p. 361, 2017.
- [33] T. M. Cover and J. A. Thomas, *Elements of information theory*. John Wiley & Sons, 2012.
- [34] G. Wang, K. Wang, C. Gong, D. Zou, Z. Jiang, and Z. Xu, "A 1mbps real-time nlos uv scattering communication system with receiver diversity over 1km," *IEEE Photonics Journal*, vol. 10, no. 2, pp. 1–13, Apr. 2018.
- [35] P. Jacquet and W. Szpankowski, "Entropy computations via analytic depoissonization," *IEEE Transactions on Information Theory*, vol. 45, no. 4, pp. 1072–1081, May 1999.